Fluorescence correlation spectroscopy on electron transfer reactions : probing inter- and intramolecular redox processes

Sen, S.

Chapter 3

Fluorescence correlation spectroscopic studies on labeled Zinc Azurin: Direct observation of intermolecular electron-transfer reactions between label and redox agents

Abstract

A detailed investigation of the products of the labeling reaction of Zinc-azurin variants with the fluorescent dye ATTO655 has been performed. Fluorescence correlation spectroscopy was performed to investigate the behavior of the labeled products under redox conditions, especially the blinking time scales and the amplitudes of non-fluorescent states of ATTO655 in labeled azurin. In this work, we have tried to understand the photoinduced electron-transfer reaction using two species: one labeled at the N-terminus and another one labeled at Lys122 position. Intermolecular electron-transfer reactions were observed between the label and the redox chemicals. Oxidizing agents had no effect on the autocorrelation functions of labeled Zn-azurin whereas the reducing agents ascorbate, hexacyanoferrate (II) caused blinking of the dye. Bimolecular reaction rates were calculated to understand the behavior of the labeled species under reducing conditions.

3.1 Introduction

In recent years it has been shown that fluorescent labeling can be used to monitor the working of oxido-reductases in detail at the single molecule level(*1*)(*2*)(*3*)(*4*)(*5*)(*6*). The only requirements are that the absorption spectrum of the protein changes with the redox state of the active center, and that the fluorescence of the dye overlaps with an absorption band of the active center so that Förster resonance energy transfer (FRET) may occur. An alternation of the redox state is then reflected in an alternation of the fluorescence intensity, as well as the fluorescence lifetime(*7*)(*8*)(*9*)(*10*)(*11*). Thus, the fluorescence time trace provides a direct record of the enzyme's activity.

The technique chosen to study the time dependence of the label emission is fluorescence correlation spectroscopy (FCS), a single-molecule technique that can be used to monitor diffusing fluorescent particles in dilute solutions. Probing small numbers of molecules at a time by FCS and statistical analysis of the data reveals dynamics otherwise obscured by ensemble averaging(*12*)(*13*)(*14*). When combined with modern hard- and software, FCS allows a time resolution in the picosecond range. In fluorescence correlation spectroscopy (FCS), the intensity fluctuations of fluorescent molecules excited by a Gaussian laser beam are studied. The fluctuations provide the autocorrelation functions, and the molecular diffusion time can easily be determined. By the introduction of extremely small detection volumes and modern hard- and software, the sensitivity of FCS has been increased tremendously. Thus, not only diffusion, but a range of dynamic processes, can be studied e.g. translational and rotational motions, chemical reactions and binding interactions. This, in turn, provides information on the phenomenon of blinking and the photophysics of a fluorophore. Blinking is commonly described by a three-state model: a ground state and the first excited singlet state, S_0, and S_1 respectively, and the lowest triplet state T_1. Owing to its longer lifetime, T_1 is considered to be the photochemically most reactive state of the dye. The presence of this state allows the fluorophore to react with other molecules and to switch between bright and dark states, i.e., to undergo blinking. This behavior of the fluorophore is responsible for intensity fluctuations. They can be analyzed by constructing the autocorrelation function (ACF) of the fluorescence-time trace. The presence of oxidizing or reducing agents in the solution can also generate blinking (*15*)(*16*)(*17*).

As a model system, the blue copper protein azurin from *Pseudomonas aeruginosa,* labeled with ATTO655, was chosen to investigate ET reactions. Azurin is a small protein (14

kDa) that is found in a variety of microorganisms and fulfills a putative role in oxidative stress-induced responses(*18*)(*19*). The metal ion can be substituted with Zn^{2+}, which changes the optical and mechanistic properties of the construct as Zn^{2+} is redox inactive. This chapter deals with the study of Zn Azurin (ZnAzu).

The zinc azurin originally is a by-product of heterologous expression azurin from *E. coli.* Zinc is probably incorporated into the protein during its expression and it is transported into the periplasm. The purified ZnAzu had been characterized by chemical analysis as well as by electrospray ionization mass spectrometry, and the structure was determined by X-ray crystallography previously(*20*). The overall structure of azurin was not perturbed by the metal exchange. However, the polypeptide structure surrounding zinc-binding site went through a small change in comparison to that in wild-type copper azurin(*20*)(*21*). Zinc azurin can also be reconstituted from copper azurin by chemical methods(*22*).

It is helpful to obtain an idea about the reactions that might contribute to the FCS signal in the case of ZnAzu. Neither FRET nor electron-transfer processes involving the metal center are expected to occur. Only intermolecular reaction between the redox chemicals and the label happens leading to redox induced blinking of the label. In the present study, it is shown that under specific redox conditions, a distortion is detected in the correlation curves, and this distortion can be attributed to the blinking of the labeled molecules under investigation (Fig. 3.1). Furthermore, by fitting the autocorrelation curves accurately, information on the rates of intermolecular ET reaction between the label and the added redox agents can be extracted. In this chapter, the prototype molecule ZnAzu, a diamagnetically blank species has been used to scrutinize the effects of redox chemicals and intermolecular ET reactions on the autocorrelation functions (ACF).

3.2 *Materials and methods*

3.2.1 *Azurin expression and purification*

Wild-type azurin (*Pseudomonas aeruginosa*) was expressed in *E.coli* and purified as previously described(*20*). Cells from *E.coli* JM109 were transformed using a pGK22 plasmid containing the azurin gene followed by a signal peptide for periplasmic translocation. After culturing in 6 liter luria broth (LB) medium till $OD_{600\ nm}$ reached 0.8 (with 0.5 mM isopropyl β-

D-1- thiogalactopyranoside, IPTG), cells were harvested and resuspended in a 20% (w/v) sucrose solution in 30 mM Tris pH 8.0 containing 1 mM EDTA for 30 min at room temperature. Thereafter the solution was centrifuged at 8000 rpm for 15 min and the supernatant-sucrose fraction was collected. Then, the cells were resuspended in Milli-Q water at 4 ºC, stirred for 30 min and centrifuged again at 8000 rpm for 15 min. Subsequently the supernatant obtained from the centrifugation process was added to the previously stored sucrose fraction while the pellet was discarded. When expressed in *E. coli*, azurin usually comes as a mixture of apo- and Zn-azurin. Therefore, after the cells were lysed, copper nitrate [$Cu(NO_3)_2$] was slowly added to the medium in order to incorporate copper in the polypeptide matrix. The final concentration of Cu was kept at ~ 1 mM. Potassium hexacyanoferrate(III) was added to the solution to a final concentration of 100 µM to produce an oxidizing environment. A stepwise precipitation was performed by lowering the pH of the solution to pH 4.0 by adding concentrated acetic acid. The precipitated protein was then removed by centrifugation at 8000 rpm for 30 min.

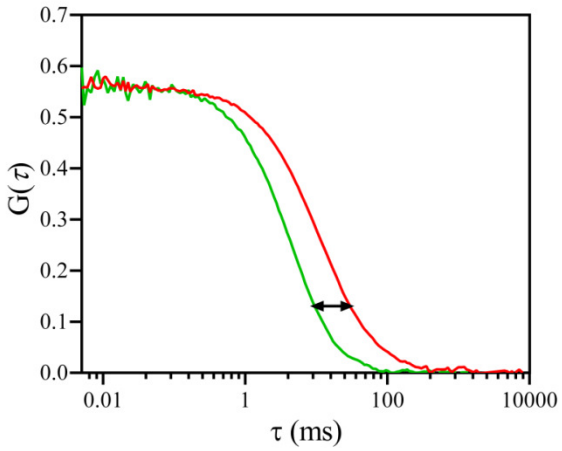

Figure 3.1: *Example of autocorrelation curves under different conditions. The red curve belongs to the FCS data of a freely diffusing labeled molecule under oxidizing conditions (500 µM potassium hexacyanoferrate (III)) and the green curve represents the same under reducing condition (500 µM potassium hexacyanoferrate (II)).*

The resulting clear supernatant solution contained azurin. It was loaded on a home packed CM Sepharose Fast Flow (GE Amersham Biosciences) column pre-equilibrated with 50 mM ammonium acetate buffer pH 4.0. Then the elution was performed using a pH gradient from pH 4.0 to pH 6.9, 50 mM ammonium acetate. Then, the fractions containing azurin were collected, pooled and the buffer was exchanged to 5 mM Tris pH 8.5. The solution was reduced

with sodium dithionite and loaded onto a home packed DEAE Sepharose Fast Flow (GE Amersham Biosciences) column. A salt gradient from 0 to 50 mM of NaCl in 5 mM Tris pH 8.0 was implemented to elute the azurin fractions. In this step, copper and zinc fractions were separated under the salt gradient. The purity of Zn azuirn fractions was checked on sodium dodecyl sulphate (SDS)-polyacrylamide gel electrophoresis (PAGE) and by means of UV/Vis spectroscopy (Cary 50 spectrophotometer, Varian Inc., Agilent Technologies, USA). The buffer of Zn azurin fractions was exchanged to 20 mM HEPES, pH 7.0 and stored at -80 ºC.

Subsequently, the copper fractions were pooled, the buffer was exchanged to 20 mM HEPES, pH 7.0 and the protein was oxidized by adding potassium hexacyanoferrate(III) upto 1.0 mM. The purity of the protein fractions was checked again on sodium dodecyl sulphate (SDS)-polyacrylamide gel electrophoresis (PAGE) and by means of UV/Vis spectroscopy. If necessary, the copper azurin containing fractions were further purified with a 5 ml HiTrap SP column (GE Healthcare) in 50 mM ammonium acetate and a pH gradient from pH 4.0 to pH 6.9 to avoid contamination of zinc azurin. All the chromatographic procedures were carried out on ÄKTA Purifier system (GE Healthcare). After the last column the final product appeared as a single band on SDS-PAGE gel with an apparent mass of ~14 kDa and showed an UV/Vis spectrum with $Abs_{628\ nm}/Abs_{280\ nm}$ ratio of ~0.57 which indicated full loading of the copper site(*20*). Labeling and FCS experiments on Cu azurin will be discussed in Chapter 4.

3.2.2 *Characterization and labeling of Zinc-Azurin*

Unless stated otherwise, chemicals were purchased from Sigma-Aldrich (Sigma-Aldrich Corp., St. Louis, USA) and used as received. Labeling experiments on ZnAzu with stoichiometric concentrations of the active form of ATTO655 dye was performed as previously described (*4*)(*23*). The labeling reactions produced a sample containing a variety of products in which the label is attached to the surface exposed Lysines as well as to the N-terminus.

3.2.3 Purification of labeled species and characterization

To obtain a homogeneous 100% singly labeled sample from the labeling solution, ion exchange chromatography (IEC) of the labeled protein was performed following the protocol mentioned earlier(*24*). Fig. 3.2A shows a chromatogram of the products of the labeling reaction of ZnAzu with ATTO655 dye, where each peak corresponds to a different species. The

chromatogram shows a similar elution profile as CuAzu (Chapter 4, Fig. 4.1). By analogy with CuAz (See Chapter 4), the peaks were analyzed as follows. Peak 1 was corresponds with ZnAzu and the peaks 2-4 can be assigned to singly labeled species where peak 2 is N-terminally labeled ZnAzu (Nt-ZnAzu) and peak 3 corresponds to the protein labeled at Lysine122 position (K122-ZnAzu). The *protein:label* stoichiometry for each peak was determined from the extinction coefficients $\mathcal{E}_{Azurin}^{280}$ = 9.8 $mM^{-1}cm^{-1}$ and $\mathcal{E}_{dye}^{663}$ = 125 $mM^{-1}cm^{-1}$ by UV/Vis spectrometry. Peak 2-4 were found to be singly labeled species. Fig. 3.2B represents Zn azurin labeled with ATTO655 at the N-terminus. The absorption spectrum of a labeled ZnAzu has been displayed in Fig. 3.3A. To verify the switching behavior of the labeled molecules, fluorescence time courses were measured in the bulk following the methods described in Chapter 2. ZnAzu is diamagnetic and redox inactive. Consequently, when it was labeled with the ATTO655 dye, the samples didn't show any fluorescence switching upon addition of oxidant and reductant (Fig. 3.3B).

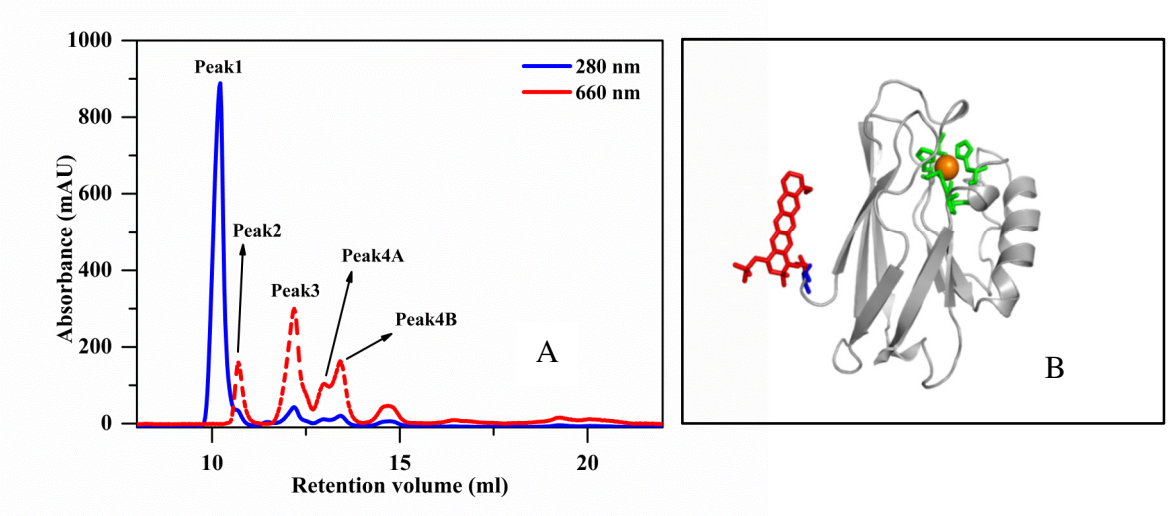

Figure 3.2: *(A) Ion exchange chromatography of the mixture obtained after labeling ZnAzu with ATTO655. The chromatogram shows the elution pattern with monitoring two wavelengths: 280 nm (blue line), characteristic absorption of the protein; and 660 nm (red line), characteristic absorption of the label. This elution is performed in 5 mM Tris, pH 8.5 with a salt gradient of 0-80 mM. The peaks have been assigned to identify the corresponding species throughout the text. (B) Schematic representation of azurin labeled with ATTO655 at the N-terminus (Nt-ZnAzu).*

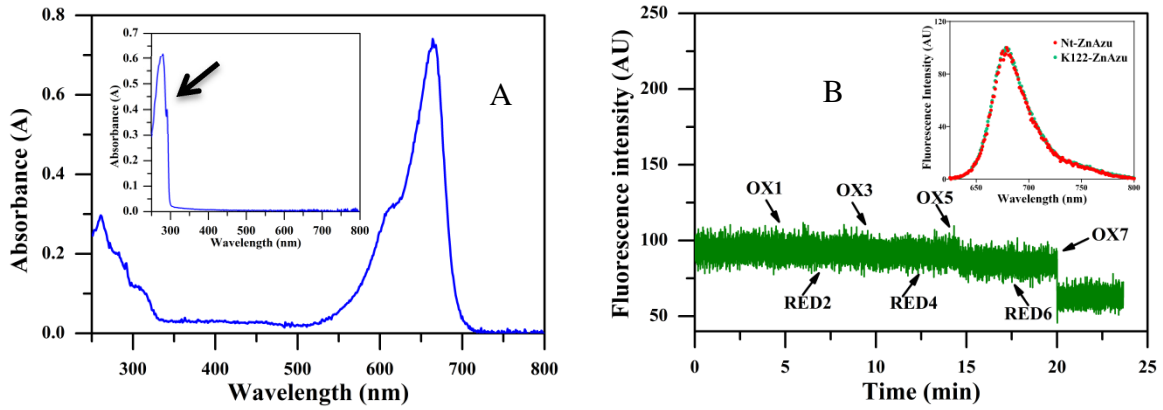

Figure 3.3: *(A) The blue curve presents the optical absorption spectrum of 6 µM solution of K122-ZnAzu labeled with ATTO655 in 20 mM HEPES pH 7.0 at room temperature. The UV/Vis spectrum of a 60 µM solution of ZnAzu in 20 mM HEPES pH 7.0 has been presented in the inset. A shoulder (black arrow) at 291 nm is the signature of the single tryptophan in azurin. (B) Fluorescence switching experiment performed on 50 nM solution of ATTO655 labeled K122-ZnAzu in 20 mM HEPES pH 7.0 at room temperature. The green trace shows the fluorescence emission at 684 nm, upon excitation at 663 nm. The arrows indicate when the chemicals were added: OX stands for the addition of oxidizing agent [Hexacyanoferrate (III)], and RED stands for the addition of reductant (Ascorbate). The OX1, OX3, OX5 and OX7 correspond to the addition of 0.05, 1, 6, and 18 mM (final concentrations) of potassium hexacyanoferrate (III) to the sample, respectively. The time points RED2, RED4, and RED 6 correspond to the addition of 0.25, 1.5, and 4.5 mM of sodium ascorbate (final concentrations) respectively. No switching was observed as expected (See text). The fluorescence trace drops after the last addition of oxidant: this is due to the dilution effect. Fluorescence spectra of 50 nM solution of Nt-ZnAzu and of K122-ZnAzu are presented in the inset of Panel B.*

3.2.4 Sample preparation for FCS experiments

FCS measurements on labeled azurin samples were performed in aqueous sucrose solution. The preparation of stock sucrose solution (75 % w/v) has been described in Chapter 2. For each measurement, a fresh sample solution was prepared by mixing 372 µl of the sucrose stock solution with 4 µl of bovine serum albumin (BSA) stock solution (10 mg/ml), 4 µl of a 100 nM azurin stock solution and between 10 and 20 µl of 2 or 20 mM freshly prepared stock solutions of ascorbate or hexacyanoferrate(II) or (III) as redox agents. The sample was adjusted to 400 µl by admixture (≤ 20 µl) of 100 mM HEPES buffer, pH 7.0. The calculated sucrose content of the samples was 57% (w/w), corresponding to a viscosity of 37.5 cP at 22^{0}C. The final sample concentration of labeled protein was around 0.4-0.8 nM. The aqueous sucrose

solutions mentioned in Table 3.1 (8, 17, 35, 50, 60 % w/v) were prepared by using 320, 267, 187, 91, 43 µl of stock sucrose solution (75% w/v) respectively. Then the solutions were adjusted to 400 µl by admixture of BSA, azurin and 100 mM HEPES buffer pH 7.0 as described previously.

In the absence of BSA, the amplitude of the FCS curve [*G(0)*] varied strongly depending on the added amount of chemicals like ascorbate or hexacyanoferrate. We suspect that azurin adsorbed at the glass surface (partly) desorbed upon changing the ionic strength or the redox conditions of the solution. This incident was not further investigated. The admixture of BSA reduced the effect presumably because the BSA covered the glass surface thus preventing adsorption of the azurin. An example of the effect of BSA on the FCS measurements is shown in Fig. 3.4. The amount of sample used for each measurement was 80 µl.

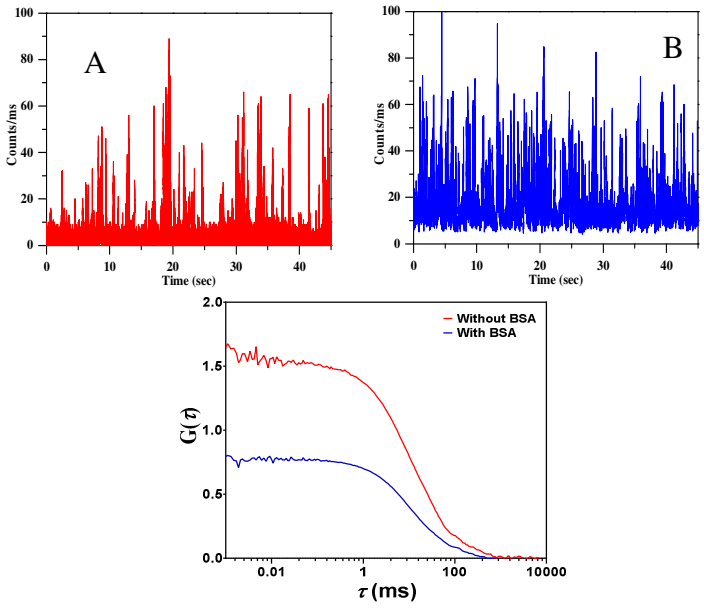

Figure 3.4: *Illustration of the effect of addition of BSA on the FCS of a 10 nM solution of azurin labeled at position K122 by ATTO655 in 57% (w/w) sucrose solution. The upper panels show the count rate as a function of time in the absence (A) and in the presence (B) of 10 mg/ml BSA. The lower panel shows the effect on the autocorrelation function: in the absence of BSA the value of G(0), which is inversely proportional to the concentration of the labeled protein, is greater than in the presence of BSA.*

3.3 Results

3.3.1 Diffusion of labeled Zinc-Azurin in sucrose solutions

To investigate the effects viscosity on the molecular diffusion, the translational diffusion times were determined by FCS for labeled ZnAzu at different sucrose concentrations in the absence of any redox chemicals. N-terminally labeled ZnAzu was chosen for this measurement, and the concentration of the labeled protein was kept at 1 nM. Seven different sucrose concentrations were used: 0, 8, 17, 35, 50, 60, 70% (w/v). For each measurement, 6 to 10 minutes of data acquisition time were required depending on the conditions of the experiments, and all the measurements were performed at room temperature (295 K).

Fig. 3.5 displays the autocorrelation function of a labeled sample in 57% w/v (70% w/v) sucrose solutions. The experiment was repeated for various sucrose concentrations. The results show that the diffusion time became longer with increase in sucrose concentrations from 0%w/w to 57% w/w. The diffusion times were foiund to be 200 µs and 12±2 ms in 0% w/v and 12±2 ms in 57% w/w sucrose solution respectively. We fitted the measured correlation functions with the following FCS equations (For details, see also Chapter 1)

$$G(\tau)=G(0)*G_{diff}(\tau) \tag{3.1}$$

$$G(0)=\frac{1}{\langle N\rangle}=\frac{1}{c\cdot V_{eff}\cdot N_A} \tag{3.2}$$

$$G_{diff}(\tau)=\left(1+\frac{\tau}{\tau_D}\right)^{-1}.\left(1+\frac{\tau}{k^2\tau_D}\right)^{-1/2} \tag{3.3}$$

The instrument parameter k = 3.5 obtained from the calibration experiments in Chapter 2 was used to fit all the autocorrelation curves (See Chapter 2). The fitting was performed in GraphPad Prism 5 (GraphPad Inc. USA) using a weighted least-square Levenberg-Marquardt method. The experimentally obtained diffusion times (Table 3.1) of labeled ZnAzu at various sucrose solutions have been used as a reference for the analysis of correlation curves for labeled CuAzu under redox conditions as a function of sucrose concentrations.

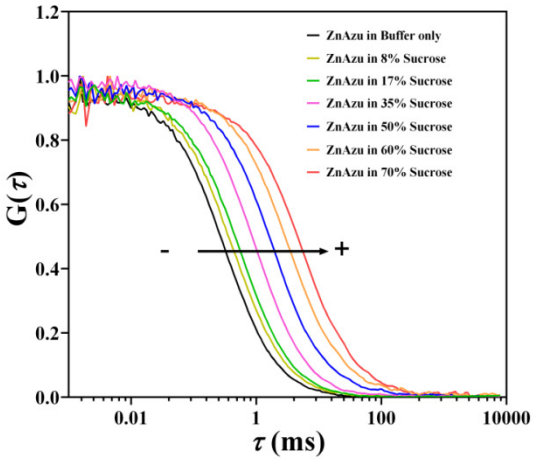

Figure 3.5: *The autocorrelation curves for N-terminally labeled ZnAzu in buffer solutions with sucrose concentration (0, 8, 17, 35, 50, 60, 70% w/v). The black arrow indicates the increase in sucrose concentrations.*

Sucrose concentration (% w/v)	Sucrose composition (%w/w)(b)	Diffusion time (τ_D), ms
0	0	0.2±0.01
8	9.4	0.4±0.03
17	21.9	0.6±.0.03
35	30.5	1.0±0.03
50	36.5	2.0±0.12
60	47.6	3.1±0.20
70	57.0	12±2.00

Table 3.1: *Experimentally obtained diffusion times (τ_D) for N-terminally labeled ZnAzu in the absence of any redox chemicals. (b) Composition of the sucrose solutions according to the tables in the CRC Handbook of Chemistry and Physics relating composition to refractive index (ref(16) and "Chapter 2, Page 38").*

3.3.2 FCS experiments under redox conditions

Single-molecule FCS experiments were performed at room temperature (295 K) in 100 mM HEPES buffer pH 7.0. Redox conditions were controlled by the addition of potassium hexacyanoferrate(III) and hexacyanoferrate(II) or sodium ascorbate as oxidant and reductant respectively.

3.3.2.1 N-terminally labeled ZnAzu (Nt-ZnAzu)

Oxidizing conditions: Fluorescence time traces were recorded of 0.5-1 nM solutions of N-terminally ATTO655 labeled ZnAz in 57% w/w (70% w/v) sucrose in the presence of varying amounts (0-500 µM) of the oxidant potassium hexacyanoferrate(III). For each time trace the autocorrelation function was calculated. An example is shown for 50 µM hexacyanoferrate(III) in Fig. 3.6. It appears that application of Eqn. 3.1 provides excellent fits of the data. The diffusion correlation time τ_D obtained from the fitting of all FCS curves (0-500 µM) is found to be independent of the $K_3Fe(CN)_6$ concentration (inset of Fig. 3.6).

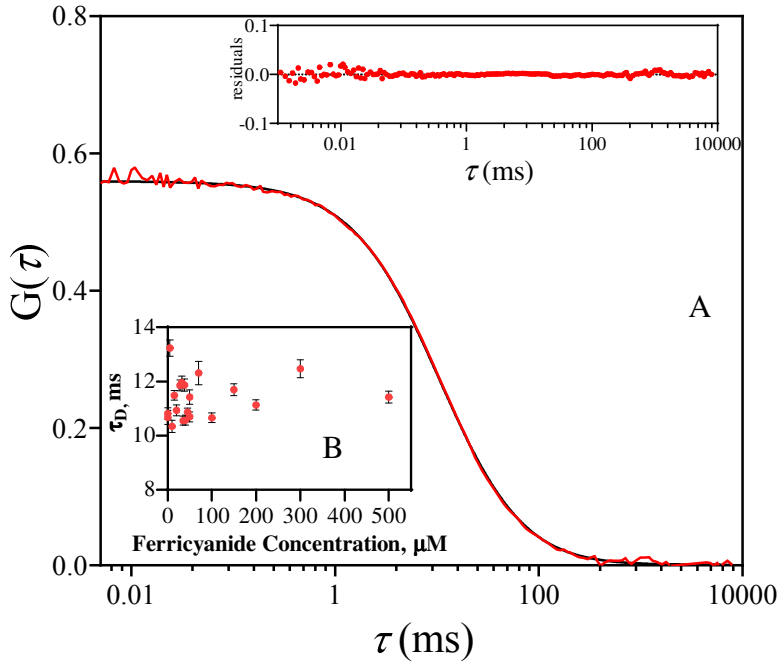

Figure 3.6: *(A) Experimentally observed ACF of 1 nM ZnAzu labeled at the N-terminus with ATTO655 in 70 % (w/v) aqueous sucrose solution of 20 mM HEPES pH 7.0 at room temperature. The sample contained 50 µM potassium hexacyanoferrate(III). The black line is a fit according to Eqn. 3.1 with G(τ) = G(0) $G_{diff}(\tau)$. The inset on top shows the residuals of the fit. (B) Diffusion times observed at various concentrations of hexacyanoferrate(III) in 70 % (w/v) aqueous sucrose solution. Vertical bars denote 95% confidence intervals.*

Reducing conditions: The observations are different when reducing conditions apply. Focusing on Nt-ZnAzu, the data obtained in the presence of freshly prepared potassium hexacyanoferrate(II) was fit with Eqn. 3.1 (only accounting for diffusion) (Fig. 3.7) and the residuals exhibited a noticeable non-random component and more importantly, τ_D varied strongly with hexacyanoferrate(II) from 12 ms at 0 µM hexacyanoferrate(II) to 2 ms at 500 µM hexacyanoferrate(II) (Fig. 3.7 D). Since this observation physically makes no sense, the ACFs were fit with an equation containing a diffusion term and a single blinking term ($G(\tau) = G(0)\ G_{diff}(\tau)\ G_1(\tau)$) (Eqn. 3.4) with the diffusion correlation time fixed at τ_D = 12 ms,

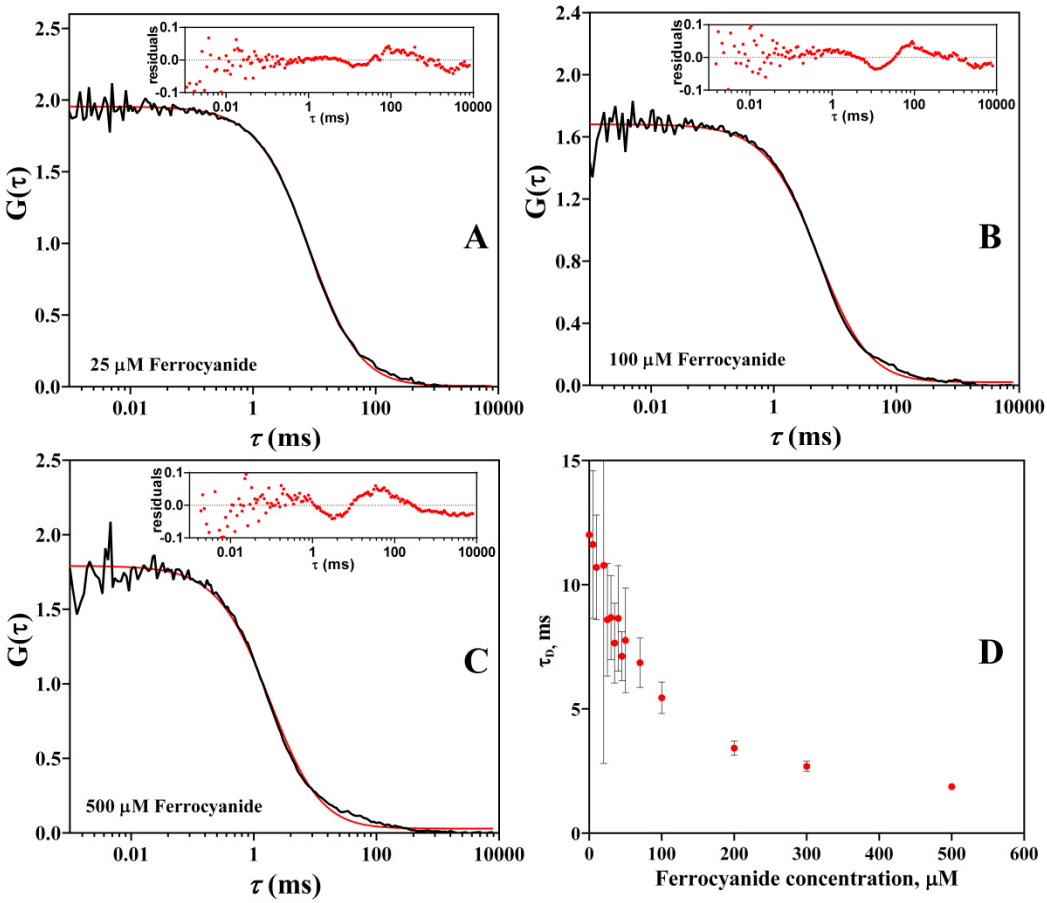

Figure 3.7: *Experimentally observed ACFs of Zn azurin labeled at the N-terminus with ATTO655 for samples containing 25 (A), 100 (B) and 500 µM (C) potassium hexacyanoferrate(II) (top to bottom). The red lines are fits according to Eqn. 3.1 with $G(\tau) = G(0)\ G_{diff}(\tau)$. The insets show the residuals of the fits. (D) Diffusion time derived from the fits for various concentrations of hexacyanoferrate(II).*

where $G_1(\tau)$ relates to zero-order reactions such as fluorophore blinking or a deprotonation

reaction; F_1 is the fraction of molecules associated with such process, and τ_1 is the relaxation time required for that reaction. Satisfactory fits were obtained now and τ_1 and F_1 can be extracted from the fitting of the FCS curves. These parameters were found to vary with reductant concentration. Fig. 3.8 displays the fitting and the residuals of FCS curves under 25, 100 and 500 µM hexacyanoferrate (II) using the FCS equation containing a blinking term as follows

$$G(\tau)=G(0)G_{diff}(\tau)G_1(\tau) \tag{3.4}$$

$$G_1(\tau)=\frac{(1-F_1+F_1e^{-\tau/\tau_1})}{(1-F_1)} \tag{3.5}$$

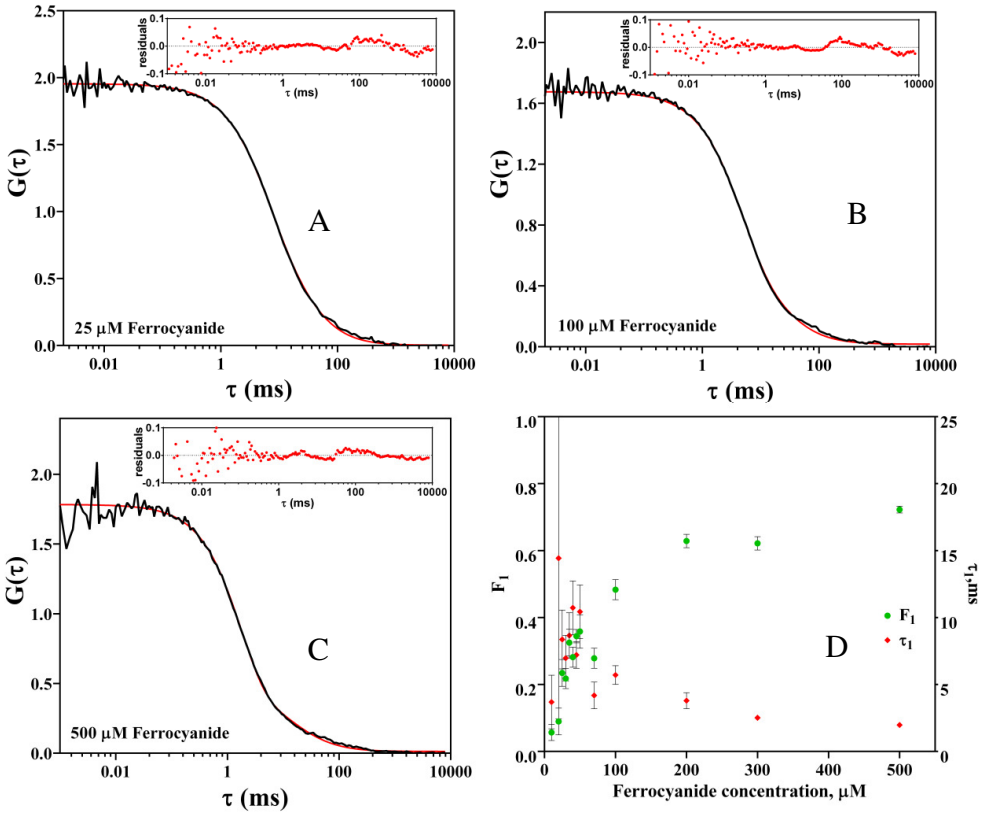

Figure 3.8: *Experimentally observed ACFs of Zn azurin labeled at the N-terminus with ATTO655 for samples containing 25 (A), 100 (B) and 500 (C) µM potassium hexacyanoferrate(II). The red lines are fits according to Eqn. 3.4 with* $G(\tau) = G(0)\ G_{diff}(\tau)\ G_1(\tau)$ *and* $\tau_D = 12$ *ms. The insets show the residuals of the fits. (D) Parameters obtained from the fits. The red squares and green circles show the values for* τ_1 *and* F_1*, and correspond with the left and right y-axis, respectively. Vertical bars denote confidence intervals.*

Similar experiments were performed with ascorbate as a reductant instead of potassium hexacyanoferrate(II). Again, τ_1 and F_1 showed a significant variation when plotted against various ascorbate concentrations (Fig. 3.9). The confidence intervals displayed in Fig. 3.9 show that in the lower reductant concentration range (0-50 µM) the experimental uncertainty is considerable, which is a general observation for almost all data sets acquired in this study. Fitting of the ACFs and their residual plots for Nt-ZnAzu under reducing conditions (0-500 µM ascorbate) are shown in Fig. 3.10.

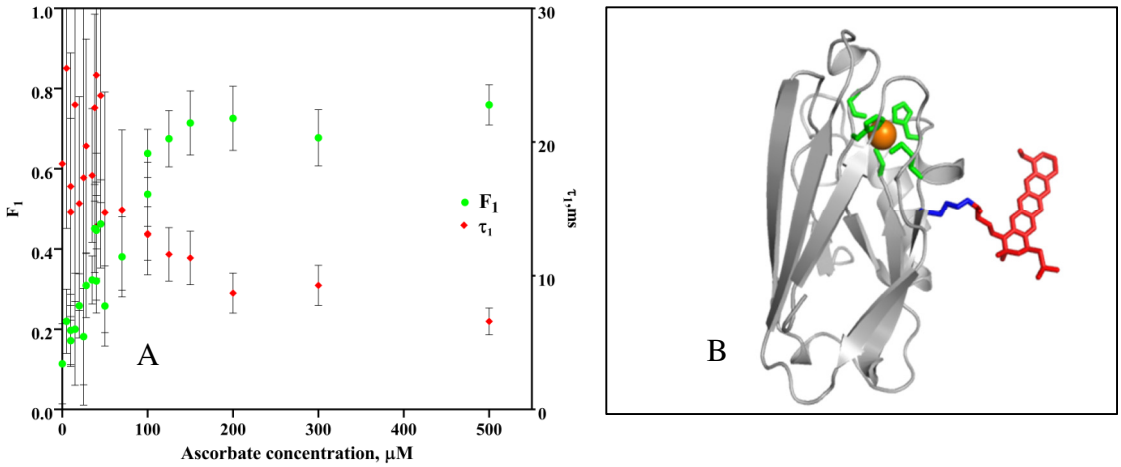

Figure 3.9: *(A) Parameters obtained from the fits from the ACFs of Zn azurin labeled at the N-terminus with ATTO655 under 0-500 µM ascorbate. The red squares and green circles show the values for τ_1 and F_1, and correspond with the left and right y-axis, respectively. Vertical bars denote confidence intervals. (B) A model representing azurin labeled with ATTO655 at position K122.*

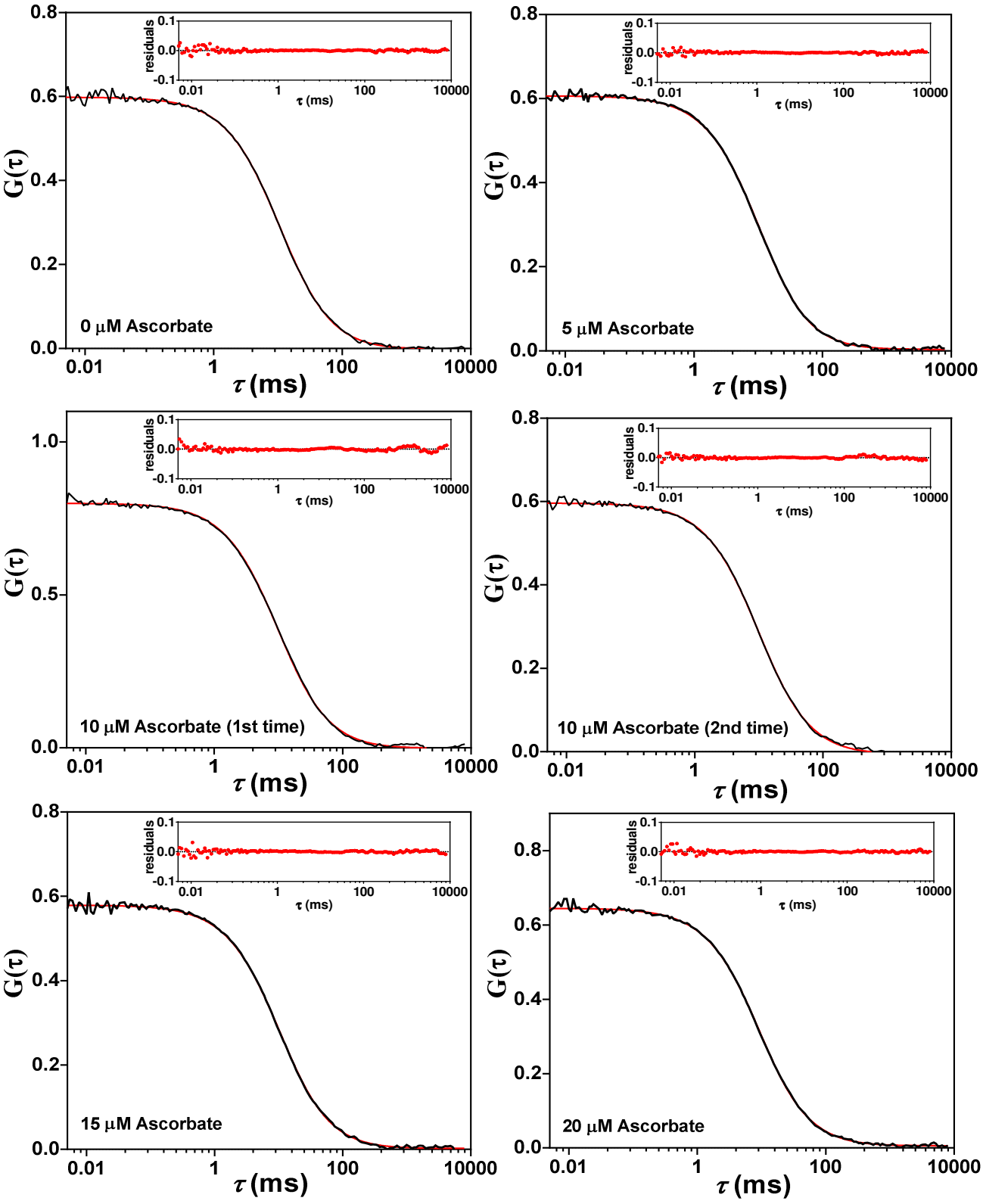
0 μM Ascorbate
5 μM Ascorbate
10 μM Ascorbate (1st time)
10 μM Ascorbate (2nd time)
15 μM Ascorbate
20 μM Ascorbate
G(τ)
τ (ms)
residuals

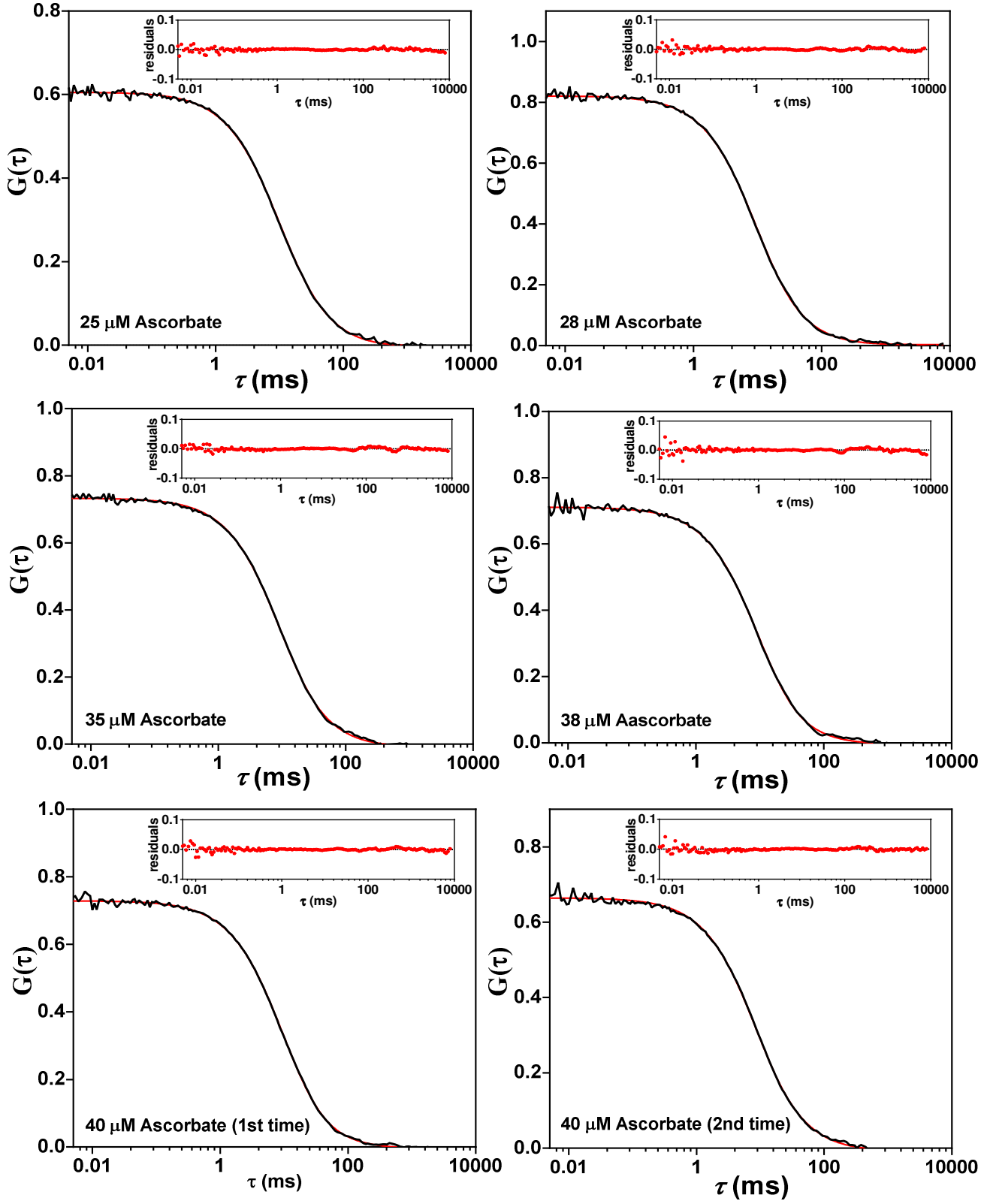
25 μM Ascorbate
28 μM Ascorbate
35 μM Ascorbate
38 μM Aascorbate
40 μM Ascorbate (1st time)
40 μM Ascorbate (2nd time)
G(τ)
τ (ms)
residuals

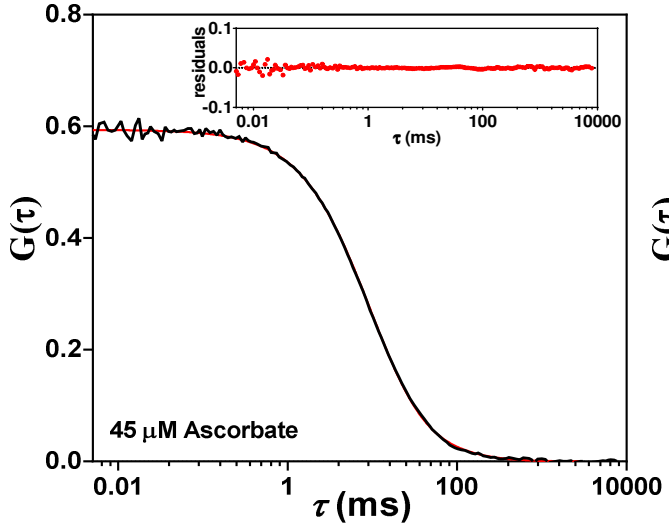
45 μM Ascorbate
G(τ)
τ (ms)
residuals

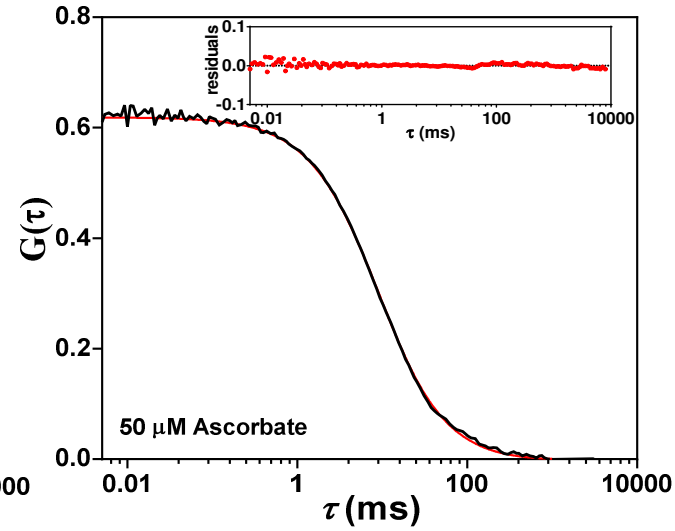
50 μM Ascorbate
G(τ)
τ (ms)
residuals

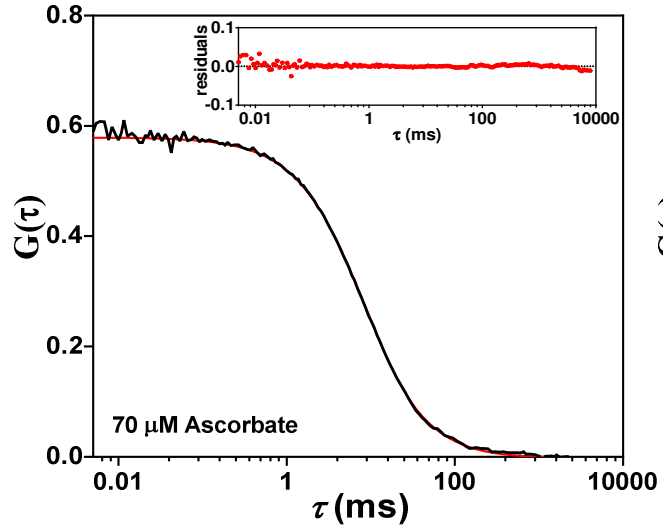
70 μM Ascorbate
G(τ)
τ (ms)
residuals

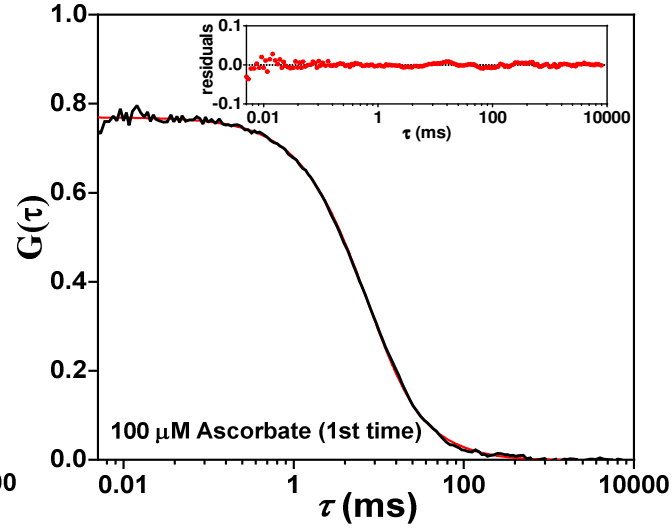
100 μM Ascorbate (1st time)
G(τ)
τ (ms)
residuals

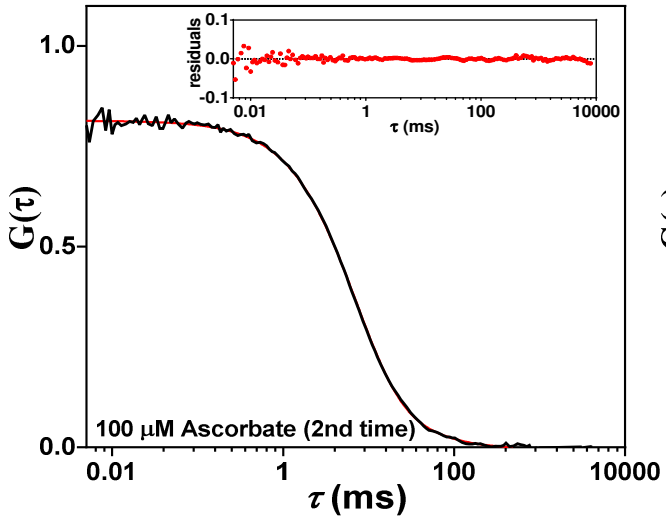
100 μM Ascorbate (2nd time)
G(τ)
τ (ms)
residuals

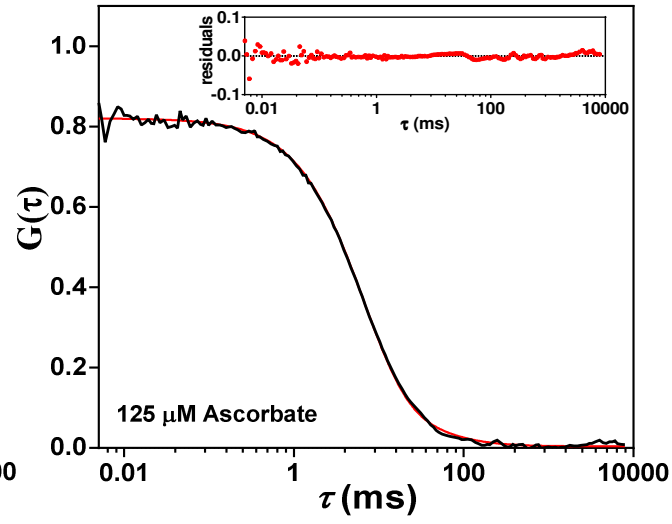
125 μM Ascorbate
G(τ)
τ (ms)
residuals

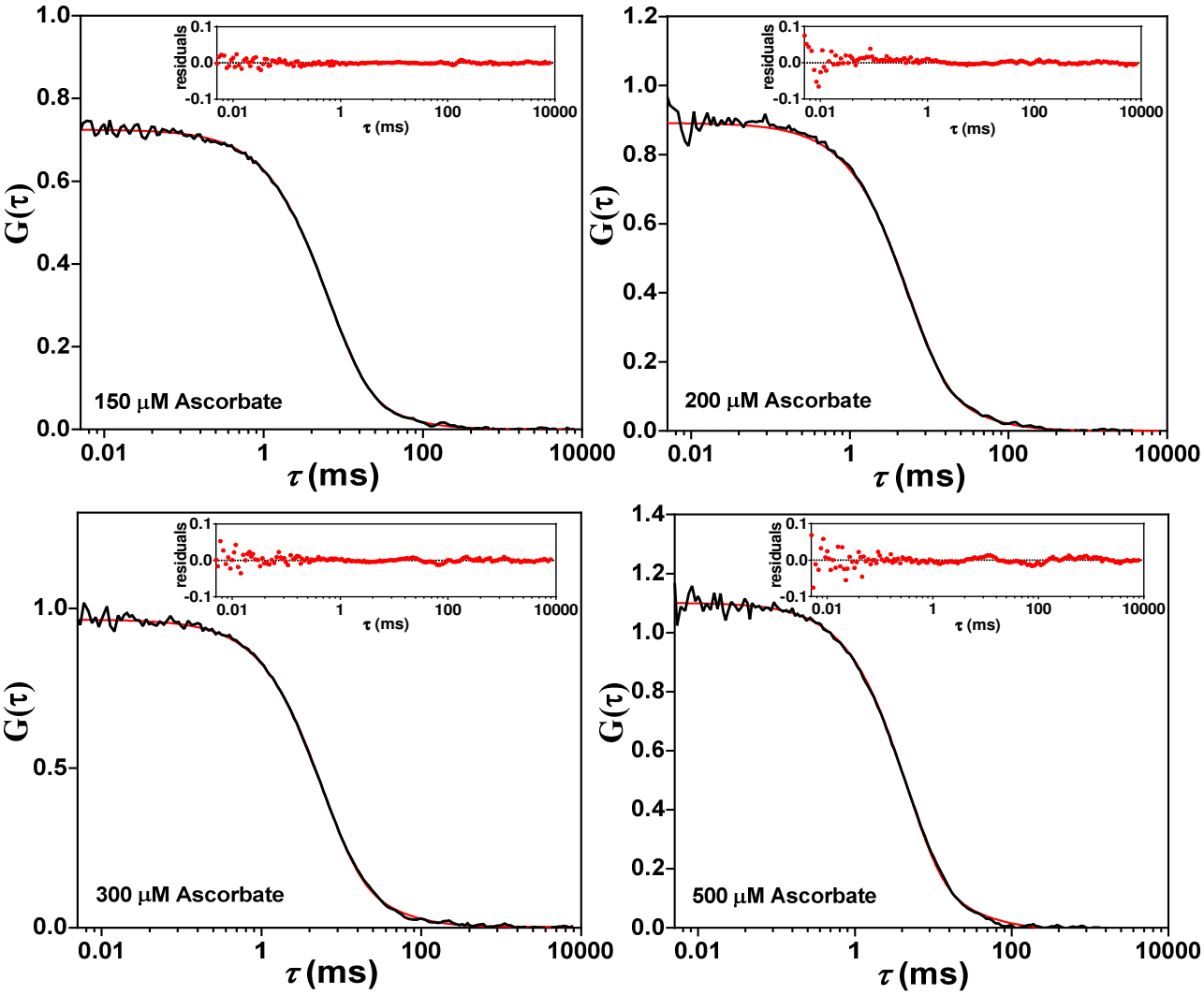

Figure 3.10: *FCS curves and residual plots for N-terminally labeled ZnAzu under reducing conditions (0-500 μM ascorbate). The red lines are fits according to Eqn. 3.4 with* $G(\tau) = G(0)\, G_{diff}(\tau)\, G_1(\tau)$ *and* $\tau_D = 12$ *ms.*

3.3.2.2 K122 labeled ZnAzu (K122-ZnAzu)

The experiments were repeated with ZnAz labeled at position 122. The results did not differ from what was observed for N-terminally labeled azurin. With hexacyanoferrate(III) as an oxidant, the autocorrelation functions could be well fit with a single diffusion term resulting in values for the diffusion correlation time between 12 and 14 ms with an average of 12.8±0.5 ms (Data presented in section 3.3.3). Under reducing conditions [hexacyanoferrate(II) or ascorbate] fitting with only a diffusion term resulted in values for τ_D that strongly varied with reductant concentration, but inclusion of a blinking term and use of a constant τ_D of 12 ms resulted in good

fits and values for τ_1 and F_1 that, again, depended on reductant concentration. The best fit of all correlation curves with their residuals is displayed in Fig. 3.11 and 3.12.

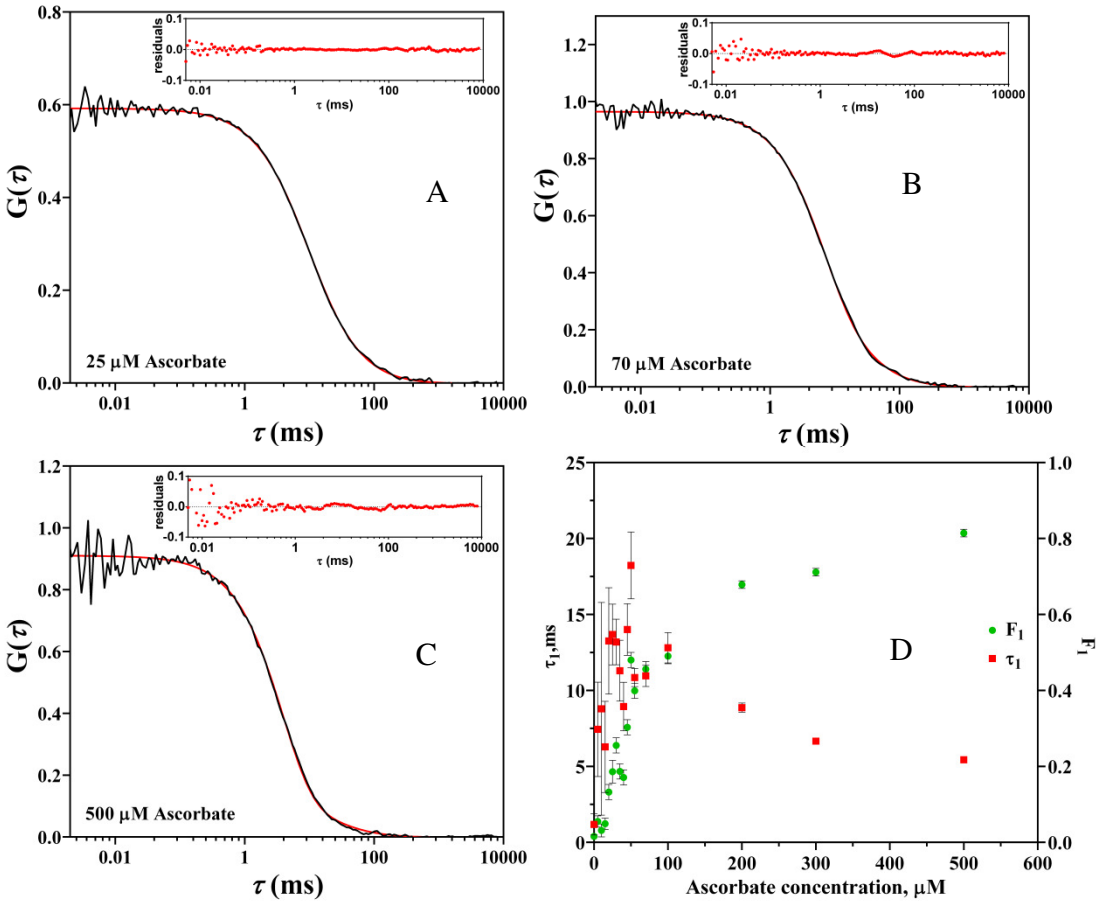

Figure 3.11: *Experimentally observed ACFs of Zn azurin labeled at the Lysine122 position with ATTO655 for samples containing 25 (A), 70 (B) and 500 (C) µM potassium hexacyanoferrate(II). The red lines are fits according to Eqn. 3.4 with* $G(\tau) = G(0)G_{diff}(\tau)G_1(\tau)$ *and* $\tau_D = 12$ *ms. The insets show the residuals of the fits. (D) Parameters obtained from the fits. The red squares and green circles show the values for* τ_1 *and* F_1*, and correspond with the left and right y-axis, respectively. Vertical bars denote 95% confidence intervals.*

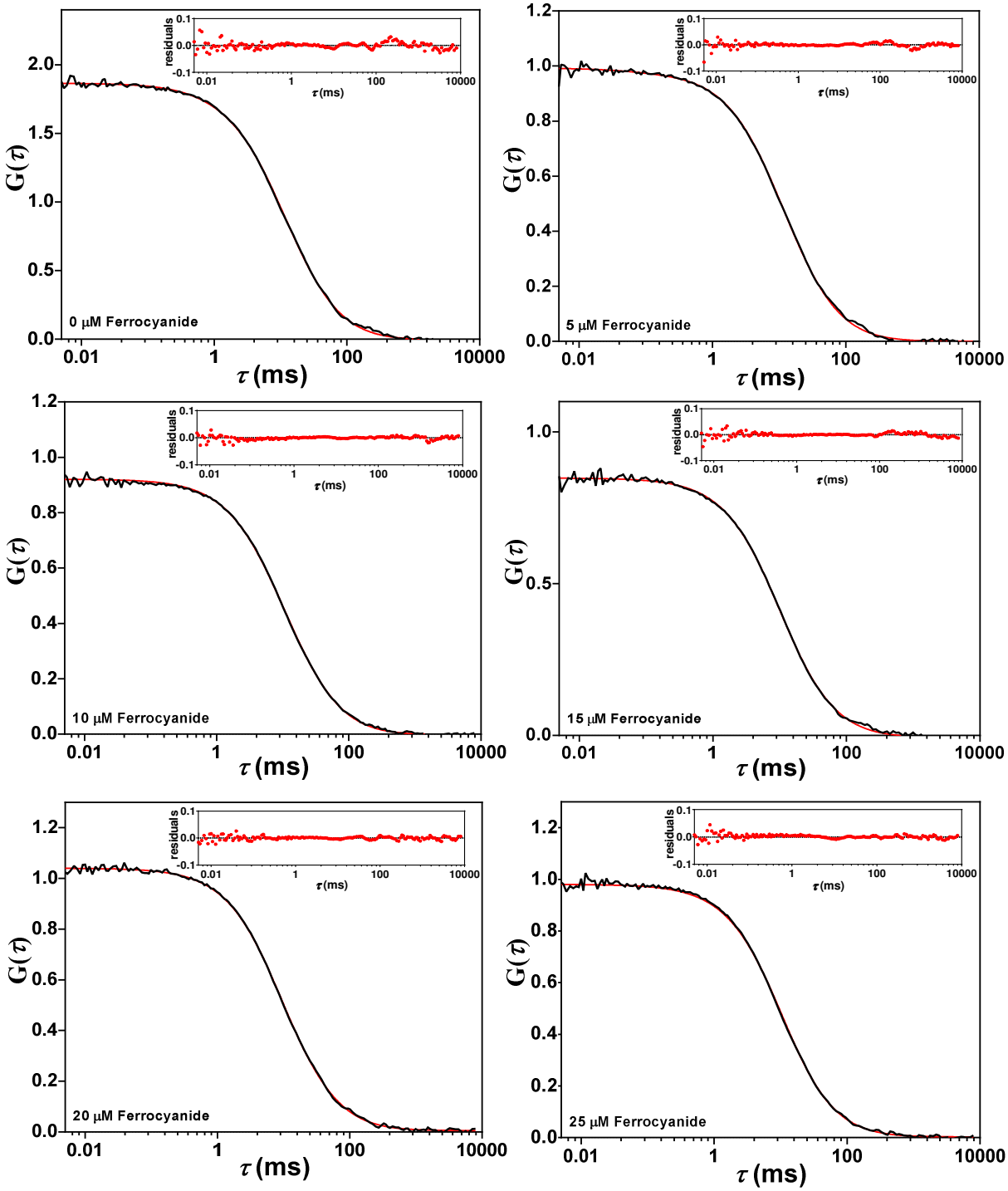
G(τ)
τ (ms)
residuals
0 μM Ferrocyanide
5 μM Ferrocyanide
10 μM Ferrocyanide
15 μM Ferrocyanide
20 μM Ferrocyanide
25 μM Ferrocyanide

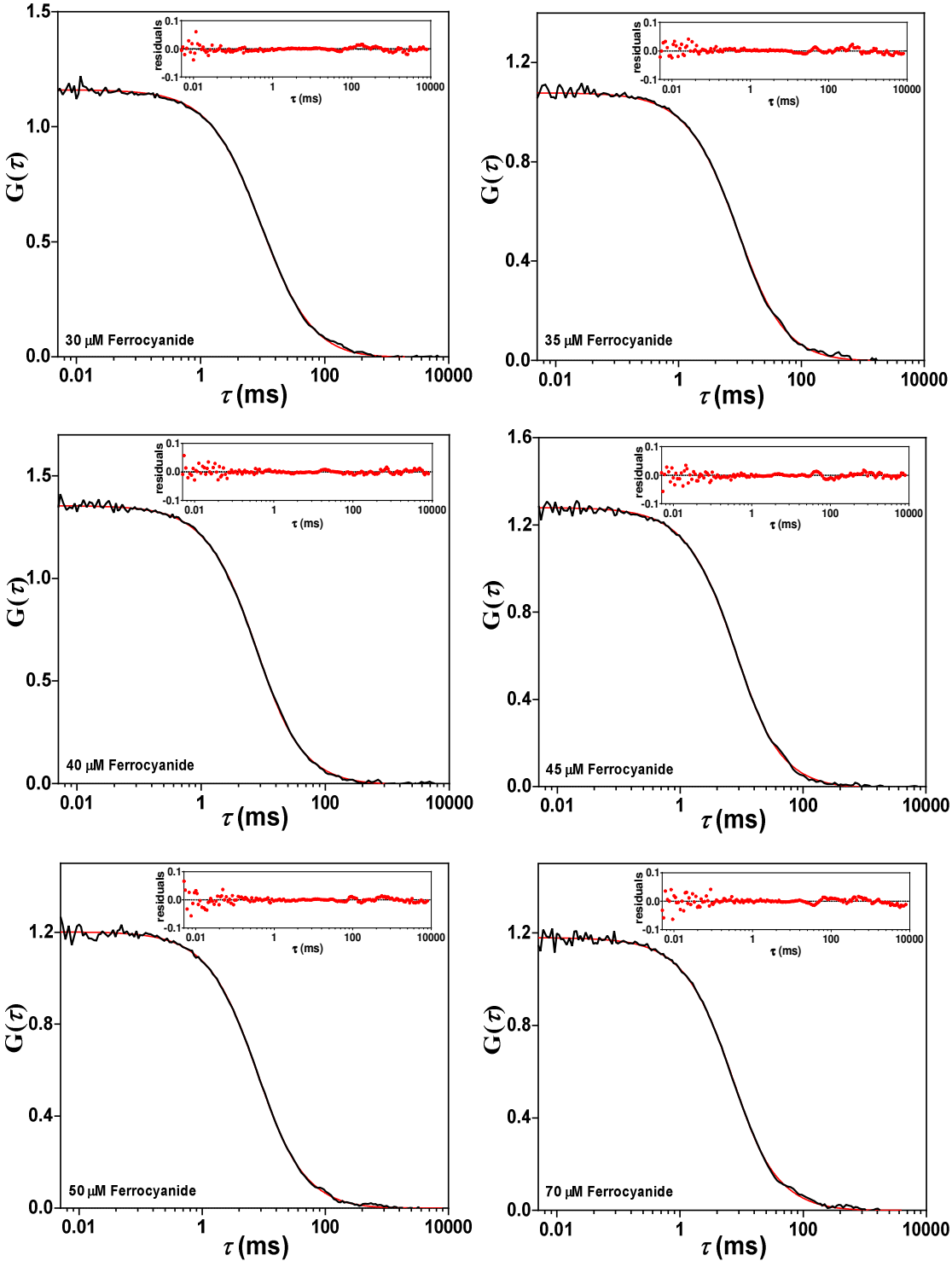
30 µM Ferrocyanide
35 µM Ferrocyanide
40 µM Ferrocyanide
45 µM Ferrocyanide
50 µM Ferrocyanide
70 µM Ferrocyanide
G(τ)
τ (ms)
residuals

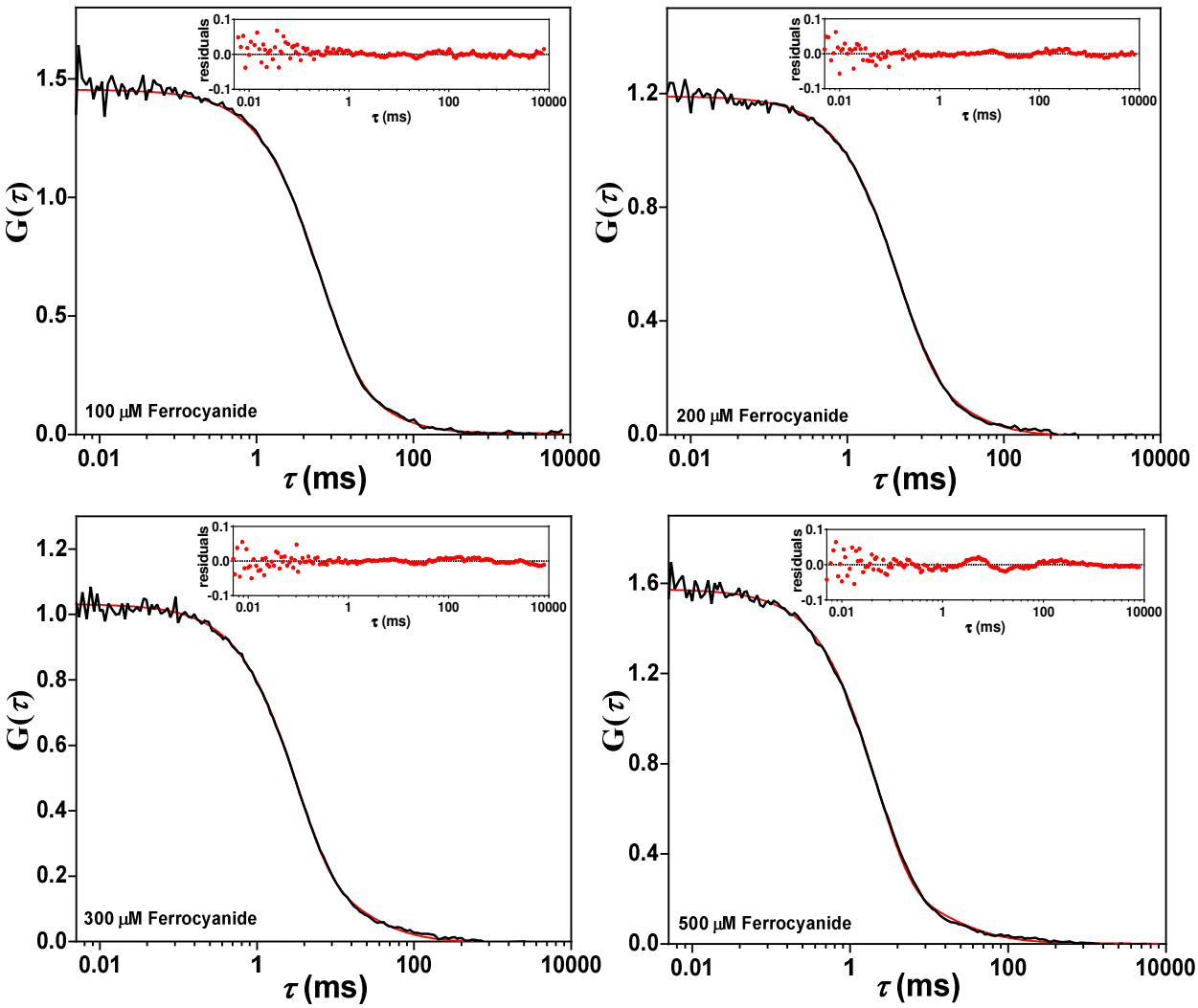

Figure 3.12: *FCS curves and residual plots for K122 labeled ZnAzu under reducing conditions [0-500 µM potassium hexacyanoferrate (II)]. The red lines are fits according to Eqn. 3.4 with* $G(\tau) = G(0)\, G_{diff}(\tau)\, G_1(\tau)$ *and* $\tau_D = 12$ *ms.*

3.4 Discussion

As ZnAzu is inactive species, only the reactions of the label with oxidants or reductants in the solution can be investigated utilizing FCS.

Redox kinetics

Oxidizing conditions: Under purely oxidizing conditions no redox kinetics could be noticed in the FCS curves of the labeled azurin (Nt-ZnAzu and K122-ZnAzu). The data obtained on the N-terminally labeled ZnAz provides a good example. Satisfactory fits of the autocorrelation traces could be obtained by using only a diffusion term in the expression for the ACF. An average τ_D of

11.3 ±0.6 ms was obtained. This value is a good agreement with the diffusion time of labeled ZnAzu mentioned previously (12±2 ms, page 76), considering the crudeness of the model used for the prediction. Clearly, at the hexacyanoferrate(III) concentrations used in this study, the label is not affected by the added oxidant. Moreover, in the FCS curves there is no sign of a photoinduced electron transfer (PET) reaction between the label and any amino side chains of the protein. Fluorescence switching experiments did not show any effect of oxidizing or reducing agents on the dye (Fig. 3.3B). The results obtained from FCS experiments, indicates that oxidizing conditions do not influence the label at the oxidant concentrations used for the single molecule experiments presented here. For Lys122 labeled ZnAz, the plot of τ_D as a function of hexacyanoferrate(III) is shown in Fig. 3.13 F, and the measured FCS curves with their residual plots have also been displayed in the following Fig. 3.13 (A-E). As similar behaviour was observed for Lys122-labeled species under oxidizing condition, it has not been further discussed.

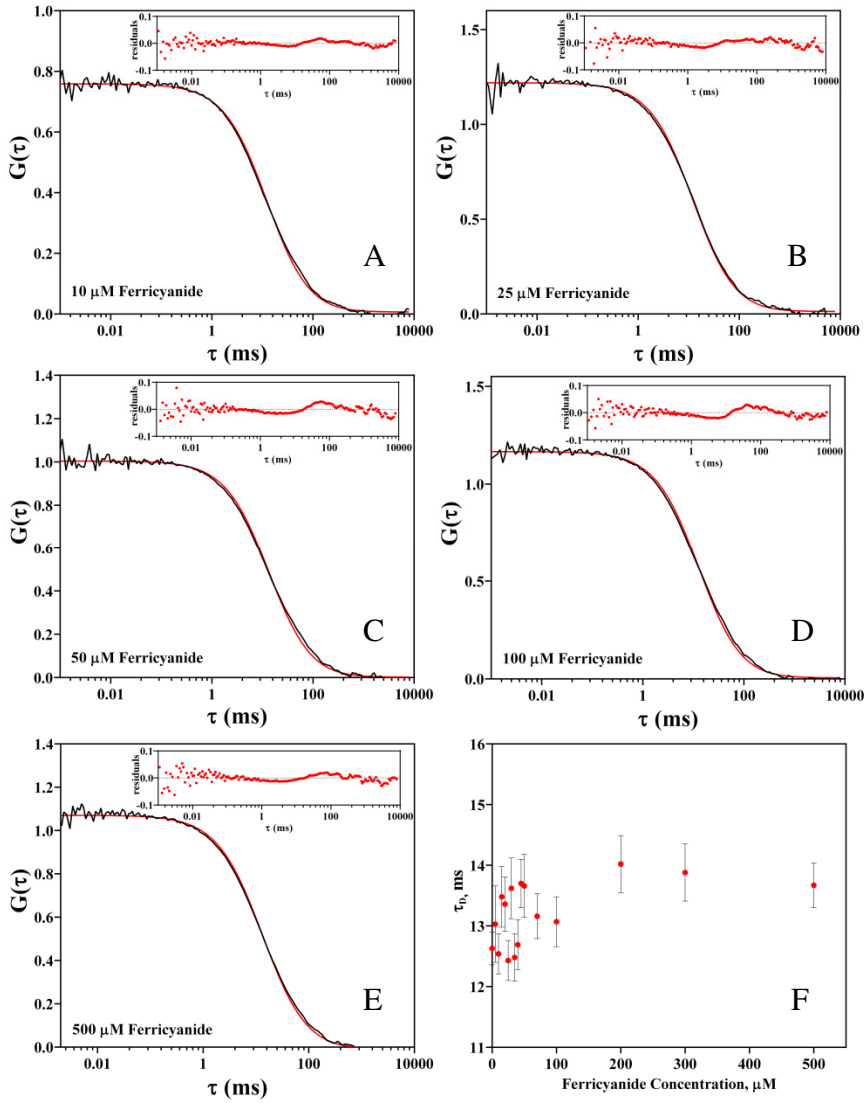

Figure 3.13: *Experimentally observed ACFs of Zn azurin labeled at the Lysine122 position with ATTO655 for samples containing 10 (A), 25 (B), 50 (C), 100 (D) and 500 (E) µM potassium hexacyanoferrate(III). The red lines are fits according to Eqn. 3.1 with G(τ) = G(0) G_{diff} (τ). The insets show the residuals of the fits. (F) Diffusion time derived from the fits for various concentrations of hexacyanoferrate(III). Vertical bars denote confidence intervals.*

Reducing conditions: Under reducing conditions the situation is different for both Nt-ZnAzu and K122-ZnAzu. A blinking term, $G_1(\tau)$, had to be introduced in the expression for the correlation function to obtain satisfactory fits of the FCS curves (Eqn. 3.4). Few examples are displayed again for K122-ZnAzu under reducing conditions (Fig. 3.14: ascorbate). The variation in

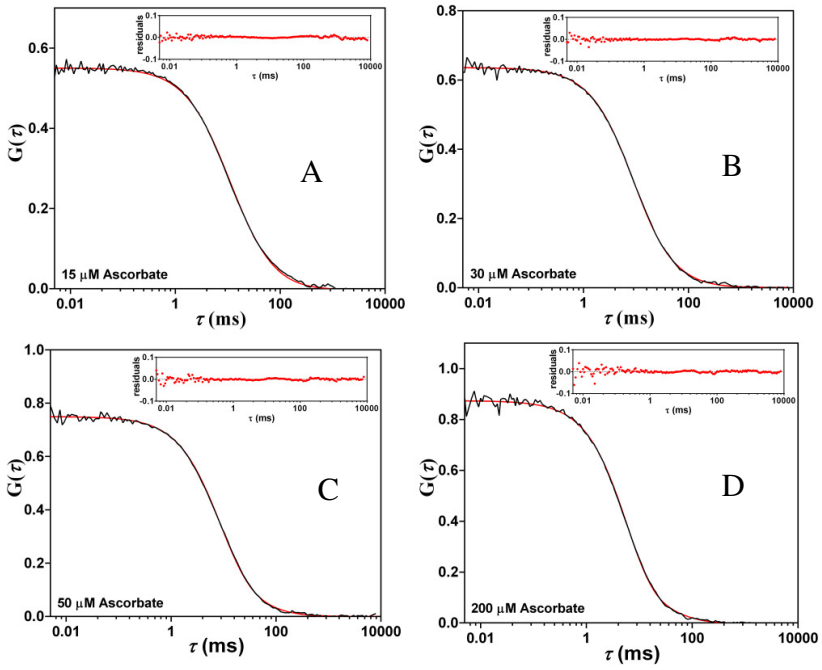

Figure 3.14: *FCS curves and residual plots for K122 labeled ZnAzu under reducing conditions 15 (A), 30 (B), 50 (C) and 200 (D) µM ascorbate. The red lines are fits according to Eqn. 3.4 with* $G(\tau) = G(0)\, G_{diff}(\tau)\, G_1(\tau)$ *with* $\tau_D = 12$ *ms.*

F_1 and τ_1 was analyzed by assuming that the label undergoes reversible transitions between bright and dark states with rate constants k_f for the transition from bright to dark and k_b for the reverse transition, i.e., the presence of ascorbate or hexacyanoferrate(II) induced blinking of ATTO655 in the solution. Expressions for F_1 and τ_1 in terms of k_f and k_b are (Scheme 3.1)

$$\text{Bright state of the dye} \underset{k_b}{\overset{k_f}{\rightleftharpoons}} \text{Dark state of the dye}$$

$$F_1 = \frac{k_f}{k_f + k_b}$$

$$\tau_1 = (k_f + k_b)^{-1}$$

Scheme 3.1: *Schematic representation of bright and dark states of the label. ATTO655 cycles between the bright and dark states under reducing conditions. The expressions of* F_1 *and* τ_1 *as function of* k_f *and* k_b *are displayed.*

The dependence of $k_f = F_1/\tau_1$ and of $k_b = (1-F_1)/\tau_1$ on reductant concentrations are shown in Fig. 3.15 and 3.16 for Nt-ZnAzu and K122-ZnAzu respectively. It is clear that k_f exhibits a linear dependence on reductant concentration; the corresponding reaction we ascribe to the one-electron reduction of the label by the reductant. The expression for k_f (*25*)(*26*);

$$k_f = k_r[R]\frac{k_{01}}{k_{10}+k_{01}} = k_r[R]f(I) \qquad (3.6)$$

Here, k_r is the second-order rate constant for the reduction of the label, [R] is the concentration of reductant, $k_{01}=\sigma I_{exc}$, with σ the absorption cross section of the label at the wavelength of the laser and I_{exc} the laser power in terms of number of photons/sec cm^2 and k_{10} is the decay rate of the excited state. The occurrence of the factor *f(I)* can be understood by considering that the optically excited label reacts with reductant in the solution on a timescale that is long compared with the excitation and fluorescence time scales (k_{01}^{-1} and k_{10}^{-1}). The reaction can then be dealt with by a two-state scheme in which the reductant is in equilibrium with a pool of labels of which only the fraction in the excited state (*f(I)*) is reactive. The slope of a graph of k_f *vs*. [R] (see Fig. 3.15 and 3.16 for Nt-ZnAzu and K122-ZnAzu respectively) provides a value of k_r *f(I)*. It amounts to 7.8×10^5 M^{-1}s^{-1} when hexacyanoferrate(II) and 2.8×10^5 M^{-1}s^{-1} when ascorbate was used as a reductant.

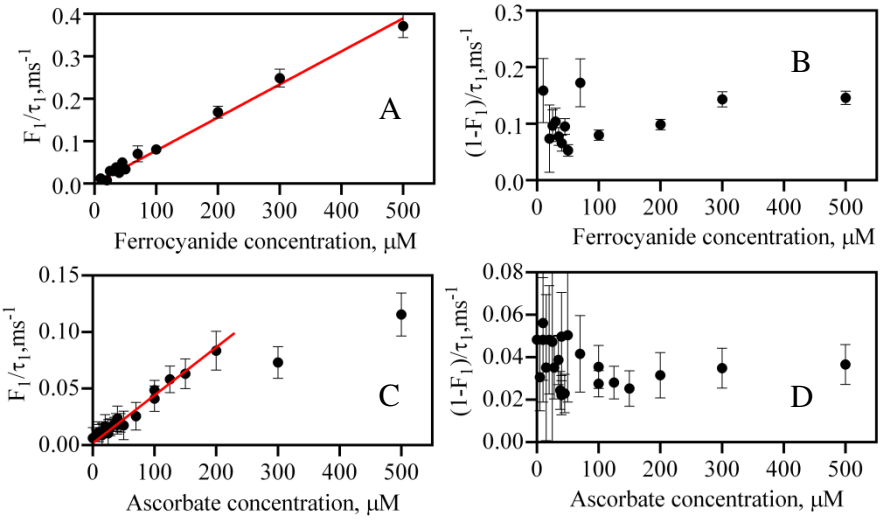

Figure 3.15: *Plots of $k_f = (F_1/\tau_1)$ and $k_b = [(1-F_1)/\tau_1]$ against the reductant concentrations for N-terminally labeled ZnAzurin. The red lines are the fit and the vertical bars indicate 95% confidence intervals.*

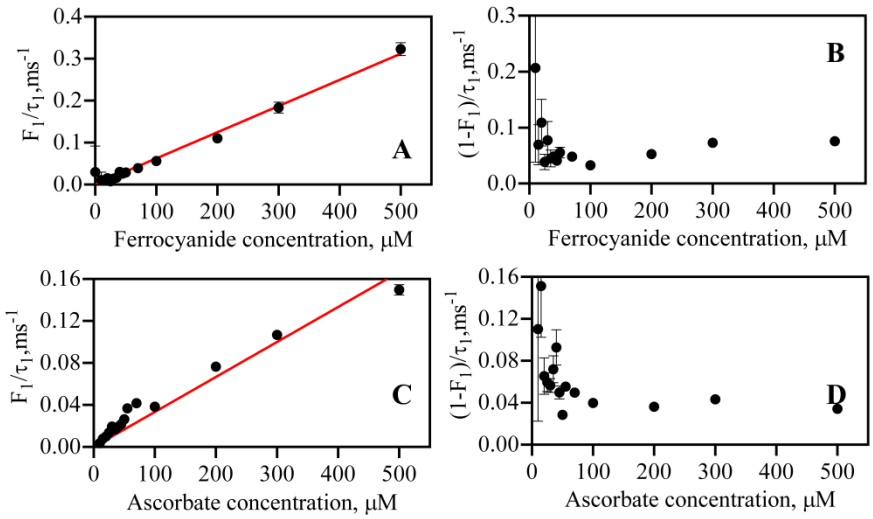

Figure 3.16: *Variations of k_f (F_1/τ_1) and k_b [$(1-F_1)/\tau_1$] as a function of reductant concentrations for Lys122 labeled ZnAzurin. The red lines are the fit and the vertical bars indicate 95% confidence intervals.*

From the experimentally determined value of $k_r f(I)$ a value of k_r can be extracted after an estimate of $f(I)$ has been obtained. With a fluorescence lifetime of 2.7 ns (See Chapter 4, measured in sucrose solution), an incident light intensity of 4.3 kW/cm^2 at 636 nm and an absorbance cross-section of the label of 1.3×10^{-16} cm^2 (based on an estimated $\varepsilon_{636} = 8\times10^4$ M^{-1}cm^{-1}), one finds that $\sigma I_{exc} = 1.80\times10^6$ s^{-1} and $f(I)=4.8\times10^{-3}$. Taking N-terminally labeled ZnAz reduced by hexacyanoferrate(II) as an example, with $k_r f(I)=7.8\times10^5$ M^{-1}s^{-1}, a value of $k_r = 1.6\times10^8$ M^{-1}s^{-1} is obtained. Considering that the experiments were performed in 70% (w/v) (i.e. 57% w/w) sucrose solutions, this is of the order of a diffusion-controlled reaction rate. Table 3.2 represents the experimental values obtained for labeled ZnAzurin under oxidizing and reducing conditions. Table 3.3 displays the values of second order rate constants for this bimolecular interaction between the label and the redox chemicals in 70% (w/v) sucrose solution. The rates are smaller compared to diffusion controlled reaction in pure buffer (10^9 M^{-1}sec^{-1}).

Intermolecular ET					
	Label at	$k_r f(I)^{(a)}$,$M^{-1}s^{-1}$	$k_r f(I)^{(b)}$, $M^{-1}s^{-1}$	$k_b^{(a)}$,s^{-1}	$k_b^{(b)}$,s^{-1}
ZnAzurin	**N-terminus**	$(7.8\pm0.2)\times10^5$	$(2.8\pm0.2)\times10^5$	$(6.0\pm0.4)\times10^1$	$(4.0\pm0.2)\times10^1$
	K122	$(6.2\pm0.3)\times10^5$	$(3.3\pm0.1)\times10^5$	$(10\pm0.9)\times10^1$	$(7.5\pm0.8)\times10^1$

Table 3.2: *Experimental values of intermolecular ET rate constants: (a) Reductant: hexacyanoferrate(II) and (b) Reductant: ascorbate.*

Label at	Reducing condition [Hexacyanoferrate(II)]	Reducing condition [Ascorbate]
N-terminus	$(1.6\pm0.04)\times10^{8}$	$(5.8\pm0.4)\times10^{7}$
K122	$(1.3\pm0.02)\times10^{8}$	$(6.8\pm0.4)\times10^{7}$

Table 3.3: *Experimental values of second order rate constants (k_r, $M^{-1}sec^{-1}$) for the bimolecular reaction between the dye and the reductants.*

In essence, such redox induced blinking is the result of the bimolecular reaction proceeding between the dye and the reductant in the sucrose solution. For labeled molecules in excited states, both oxidation and reduction reactions are possible: either an electron promoted to the LUMO is removed more easily so that the dark state has a lower oxidation potential than the ground state or the highest occupied molecular orbital when singly occupied, can accept an electron more easily than the ground state (Fig. 3.17). In the present case, the oxidant hexacyanoferrate(III) did not result in any blinking, but collisions of the excited fluorophore with electron donors e.g. ascorbate or hexacyanoferrate(II) easily led to the reduction, yielding radical ions. The radical ions stay in the stable dark states.

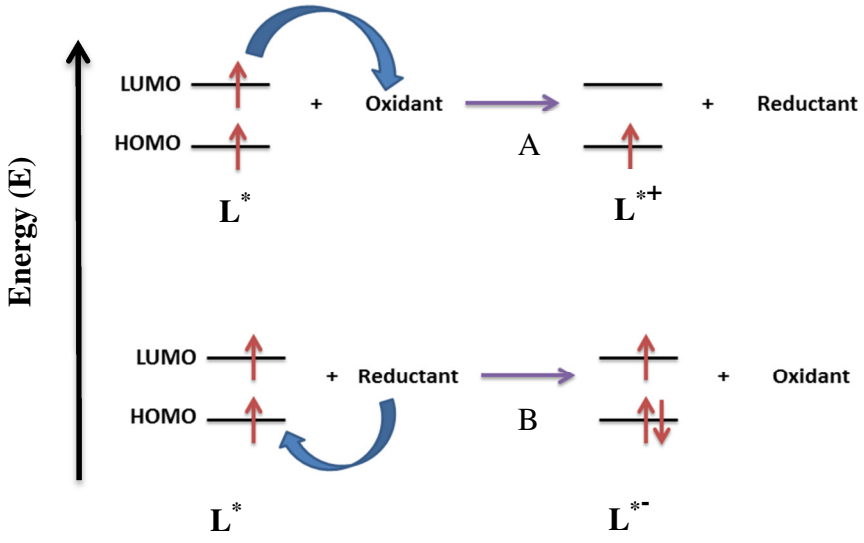

Figure 3.17: A simplified *HOMO/LUMO energy level presentation of a labeled molecule. L^* represents the molecule in the excited state, L^{*+} represents the one electron oxidized state of the label and L^{*-} corresponds to the one electron reduced form of the label. (A): single electron removed from the LUMO by the oxidizing agent; (B): one electron is added to the HOMO of the label by the reductant.*

There are non-absorbing fluorophores which are most likely long-lived radical ions. As for the oxidation of the reduced label back to the non-reduced form, the contribution of the blinking term $G_1(\tau)$ to the autocorrelation function is small at low reductant concentrations and the spread in k_b (the back reaction) is relatively large (Fig. 3.15 B and D for Nt-ZnAzu). These reactions are in microsecond up to millisecond time scale with concentration-dependent manner. It is clear that k_b does not vary systematically with the reductant concentration. Average values of k_b are listed in Table 3.2. That k_b appears to be constant is consistent with the idea that dissolved oxygen is responsible for the back oxidation of the label as oxygen is present in the solution in large excess and its concentration will not change appreciably over the duration of the experiment. When assuming that the reaction with oxygen is second order with rate k_0, one finds with k_b = 95 s^{-1} (Fig. 3.15 B and Table 3.1) and $[O_2] \approx 260$ μM (aerobic solution) that $k_0 = 3.6\times10^5$ $M^{-1}s^{-1}$. The diffusion controlled k_0 can be well understood by k_d (see Chapter 2 for details). Reaction between the labeled protein and oxygen represents the bimolecular reaction between two reactants that is expected to take place with a diffusion-controlled rate constant k_d in most solvents. Since, the label is at the surface of the protein and flexible, it can move or rotate faster than the whole protein. Oxygen molecules rapidly diffuse and react with the labeled protein. In 57% w/w sucrose solution, the bimolecular reactions between them slow down. k_0 is found to be one order of magnitude smaller than the predicted value of k_d for the present system (10^6 $M^{-1}s^{-1}$) in viscous solvent (see Chapter 2 for details), suggesting only fraction of the bimolecular encounters between the labeled protein and oxygen molecules give rise to succesful oxidation of the reduced label. Reduced form of the dye is also known to have higher reduction potential than that of oxygen such that reaction with oxygen is insufficient(*27*). Similar behavior was observed for K122-labeled ZnAz (Fig. 3.16 B and Table 3.1).

$$\text{Dark state (reduced form of the dye)} + O_2 \xrightarrow{k_0} \text{Non-reduced form}$$

3.5 ***Concluding remarks***

In the present work a single-molecule based approach to the study of intermolecular electron-transfer processes in a labeled protein is presented. The time scale of intermolecular processes depends on the viscosity of the solution. Oxidizing conditions do not show any effect on the label, but reducing agents ascorbate and potassium hexacyanoferrate (II) affect markedly and the blinking processes are observed. The excited label does react with the redox active

components in the solution in a diffusion-controlled manner. Analysis of autocorrelation data produced rate constants for bimolecular reductive quenching of the excited dye by ascorbate and hexacyanoferrate(II). The diffusion rates were diminished by two orders of magnitude by increasing the viscosity.

References

(1) Goldsmith, R. H.; Tabares, L. C.; Kostrz, D.; Dennison, C.; Aartsma, T. J.; Canters, G. W.; Moerner, W. E. Redox cycling and kinetic analysis of single molecules of solution-phase nitrite reductase. *Proc. Natl. Acad. Sci. U. S. A.* **2011**, *108*, 17269–74.

(2) Gustiananda, M.; Andreoni, A.; Tabares, L. C.; Tepper, A. W. J. W.; Fortunato, L.; Aartsma, T. J.; Canters, G. W. Sensitive detection of histamine using fluorescently labeled oxido-reductases. *Biosens. Bioelectron.* **2012**, *31*, 419–25.

(3) Kuznetsova, S.; Zauner, G.; Aartsma, T. J.; Engelkamp, H.; Hatzakis, N.; Rowan, A. E.; Nolte, R. J. M.; Christianen, P. C. M.; Canters, G. W. The enzyme mechanism of nitrite reductase studied at single-molecule level. *Proc. Natl. Acad. Sci. U. S. A.* **2008**, *105*, 3250–3255.

(4) Kuznetsova, S.; Zauner, G.; Schmauder, R.; Mayboroda, O. A.; Deelder, A. M.; Aartsma, T. J.; Canters, G. W. A Förster-resonance-energy transfer-based method for fluorescence detection of the protein redox state. *Anal. Biochem.* **2006**, *350*, 52–60.

(5) Salverda, J. M.; Patil, A. V.; Mizzon, G.; Kuznetsova, S.; Zauner, G.; Akkilic, N.; Canters, G. W.; Davis, J. J.; Heering, H. A.; Aartsma, T. J. Fluorescent Cyclic Voltammetry of Immobilized Azurin: Direct Observation of Thermodynamic and Kinetic Heterogeneity. *Angew. Chemie Int. Ed.* **2010**, *49*, 5776–5779.

(6) Patil, A. V.; Davis, J. J. Visualizing and tuning thermodynamic dispersion in metalloprotein monolayers. *J. Am. Chem. Soc.* **2010**, *132*, 16938–16944.

(7) Schmauder, R.; Librizzi, F.; Canters, G. W.; Schmidt, T.; Aartsma, T. J. The oxidation state of a protein observed molecule-by-molecule. *Chemphyschem* **2005**, *6*, 1381–6.

(8) Schmauder, R.; Alagaratnam, S.; Chan, C.; Schmidt, T.; Canters, G. W.; Aartsma, T. J.

Sensitive detection of the redox state of copper proteins using fluorescence. *J. Biol. Inorg. Chem.* **2005**, *10*, 683–7.

(9) Strianese, M.; Zauner, G.; Tepper, A. W. J. W.; Bubacco, L.; Breukink, E.; Aartsma, T. J.; Canters, G. W.; Tabares, L. C. A protein-based oxygen biosensor for high-throughput monitoring of cell growth and cell viability. *Anal. Biochem.* **2009**, *385*, 242–248.

(10) Tabares, L. C.; Kostrz, D.; Elmalk, A.; Andreoni, A.; Dennison, C.; Aartsma, T. J.; Canters, G. W. Fluorescence lifetime analysis of nitrite reductase from Alcaligenes xylosoxidans at the single-molecule level reveals the enzyme mechanism. *Chemistry* **2011**, *17*, 12015–9.

(11) Zauner, G.; Lonardi, E.; Bubacco, L.; Aartsma, T. J.; Canters, G. W.; Tepper, A. W. J. W. Tryptophan-to-dye fluorescence energy transfer applied to oxygen sensing by using type-3 copper proteins. *Chem. - A Eur. J.* **2007**, *13*, 7085–7090.

(12) Haustein, E.; Schwille, P. Ultrasensitive investigations of biological systems by fluorescence correlation spectroscopy. *Methods* **2003**, *29*, 153–166.

(13) Haustein, E.; Schwille, P. Fluorescence correlation spectroscopy: novel variations of an established technique. *Annu. Rev. Biophys. Biomol. Struct.* **2007**, *36*, 151–69.

(14) Krichevsky, O. Fluorescence correlation spectroscopy : the technique. *Rep.Prog.Phys* **2002**, *65*, 251.

(15) Ha, T.; Tinnefeld, P. Photophysics of Fluorescence Probes for Single Molecule Biophysics and Super-Resolution Imaging. *Annu Rev Phys Chem* **2012**, *63*, 595–617.

(16) Ha, T.; Tinnefeld, P. Photophysics of Fluorescent Probes for Single-Molecule Biophysics and Super-Resolution Imaging. *Annu. Rev. Phys. Chem.* **2012**, *63*, 595–617.

(17) Stennett, E. M. S.; Ciuba, M. a; Levitus, M. Photophysical processes in single molecule organic fluorescent probes. *Chem. Soc. Rev.* **2014**, *43*, 1057–75.

(18) Wilson, M. T.; Greenwood, C.; Brunori, M.; Antonini, E. Electron transfer between azurin and cytochrone c-551 from Pseudomonas aeruginosa. *Biochem. J.* **1975**, *145*, 449–457.

(19) E. T. Adman andL. H. Jensen Structural Features of Azurin at 2.7 Å Resolution. *Isr. J. Chem.* **1981**, *21*, 8–12.

(20) Van de Kamp, M.; Hali, F. C.; Rosato, N.; Agro, A. F.; Canters, G. W. Purification and characterization of a non-reconstitutable azurin, obtained by heterologous expression of the Pseudomonas aeruginosa azu gene in Escherichia coli. *Biochim. Biophys. Acta* **1990**, *1019*, 283–292.

(21) Nar, H.; Huber, R.; Messerschmidt, A.; Filippou, a C.; Barth, M.; Jaquinod, M.; van de Kamp, M.; Canters, G. W. Characterization and crystal structure of zinc azurin, a by-product of heterologous expression in Escherichia coli of Pseudomonas aeruginosa copper azurin. *Eur. J. Biochem.* **1992**, *205*, 1123–1129.

(22) Van Amsterdam, I. M. C.; Ubbink, M.; Einsle, O.; Messerschmidt, A.; Merli, A.; Cavazzini, D.; Rossi, G. L.; Canters, G. W. Dramatic modulation of electron transfer in protein complexes by crosslinking. *Nat. Struct. Biol.* **2002**, *9*, 48–52.

(23) Nicolardi, S.; Andreoni, A.; Tabares, L. C.; Van Der Burgt, Y. E. M.; Canters, G. W.; Deelder, A. M.; Hensbergen, P. J. Top-down FTICR MS for the identification of fluorescent labeling efficiency and specificity of the Cu-protein azurin. *Anal. Chem.* **2012**, *84*, 2512–20.

(24) Nicolardi, S.; Andreoni, A.; Tabares, L. C.; van der Burgt, Y. E. M.; Canters, G. W.; Deelder, A. M.; Hensbergen, P. J. Top-down FTICR MS for the identification of fluorescent labeling efficiency and specificity of the Cu-protein azurin. *Anal. Chem.* **2012**, *84*, 2512–20.

(25) Widengren, J.; Rigler, R.; Mets, U. Triplet-state monitoring by fluorescence correlation spectroscopy. *J. Fluoresc.* **1994**, *4*, 255–8.

(26) Widengren, J.; Mets, U.; Rigler, R. Fluorescence correlation spectroscopy of triplet states in solution: a theoretical and experimental study. *J. Phys. Chem.* **1995**, *99*, 13368–13379.

(27) Holleman AF *Lehrbuch der Anorgnischen Chemie*; de Gruyter: New York, 1995.